

Dissolution of residual tetrachloroethylene in fractional wettability porous media: correlation development and application

Scott A. Bradford^{*}, Thomas J. Phelan, Linda M. Abriola

University of Michigan, Department of Civil and Environmental Engineering, 181 EWRE, 1351 Beal Avenue, Ann Arbor, MI 48109-2125, USA

Received 11 August 1999; received in revised form 20 December 1999; accepted 10 January 2000

Abstract

This work explores the dissolution behavior of residual tetrachloroethylene (PCE) in chemically heterogeneous soils. A numerical solute transport simulator, that incorporates rate-limited dissolution and desorption using linear driving force expressions, was developed and applied to analyze soil column dissolution data and to conduct numerical dissolution experiments. Published mass transfer coefficients were unable to accurately predict the observed dissolution of entrapped PCE in fractional wettability porous media (media containing both water- and PCE-wet solid surfaces). A two-parameter power function expression for the lumped mass transfer coefficient was developed and successfully fit to these data. Correlations were then developed for the fitted mass transfer model parameters as a function of wettability and grain size distribution characteristics. The power function model, in conjunction with the parameter correlations, yielded reasonable predictions for long-term dissolution behavior in the more PCE-wetting media. Poorer predictions for the more water-wet materials were attributed to an increased sensitivity of effluent concentration behavior to temporal changes in PCE saturation in these systems. Many of the effluent concentration curves exhibited low and persistent concentration tailing after recovery of the separate phase PCE. This tailing behavior could be adequately modeled by incorporation of rate-limited desorption. Results from numerical experiments indicate that both the magnitude and spatial distribution of wettability can significantly influence PCE dissolution behavior and remediation time. © 2000 Elsevier Science B.V. All rights reserved.

Keywords: Dissolution; Wettability; Sorption; Nonaqueous phase liquid (NAPL)

^{*} Corresponding author. Present address: George E. Brown Jr., Salinity Laboratory, USDA, ARS, 450 W. Big Springs Road, Riverside, CA 92507-4617, USA. Tel.: +1-909-369-4857; fax: +1-909-342-4963.

E-mail address: sbradford@usse.ars.usda.gov (S.A. Bradford).

1. Introduction

The uncontrolled release of relatively insoluble organic contaminants into the subsurface has led to the widespread contamination of groundwater resources. Remediation of subsurface sites contaminated with these nonaqueous phase liquids (NAPLs) has typically involved removing as much separate phase NAPL as possible through pumping and then flushing with water in an effort to dissolve the small volume fraction of organic that remains entrapped by capillary forces (Testa and Winegardner, 1991). This “pump-and-treat” approach to subsurface cleanup tends to be inefficient, due to rate-limited interphase mass transfer and low aqueous phase solubility of many organic compounds (Mercer et al., 1990; Mackay and Cherry, 1989; Kavanaugh, 1996). Accurate predictions of NAPL persistence and the design of effective remediation strategies for NAPL contaminated sites will ultimately depend on our knowledge of the processes that control the interphase mass transfer rates of residual NAPL contaminants.

Most previous NAPL dissolution investigations have been conducted for water-wet porous media and glass beads (e.g., Hunt et al., 1988; Geller and Hunt, 1993; Miller et al., 1990; Powers et al., 1994a,b; Imhoff et al., 1994, 1997, 1998). Under water-wetting conditions, water fills the smaller pores and exists in the larger pores as continuous films coating the solid surfaces, and surrounding the residual organic liquid. The organic liquid may be entrapped within pores as relatively simple spherical singlets and/or very complex multipore ganglia. In soil column experiments with water-wet sands and glass beads, entrapped NAPL saturations typically range from 10% to 35% of the pore space (Wilson et al., 1990; Powers et al., 1992, 1994a,b).

Experimental and numerical studies have revealed that rate-limited dissolution in water-wet media can occur under many conditions; i.e., in graded media, under high aqueous phase velocity conditions, at low NAPL saturations, when the soluble component represents a small mass fraction of the NAPL, and when residual NAPL is found in “inaccessible” pores (Hunt et al., 1988; Borden and Kao, 1992; Powers et al., 1992). Linear driving force models, quasi-steady state approximations of Fick’s first law of diffusion, have typically been used to describe this rate-limited mass transfer behavior (Geller and Hunt, 1993; Imhoff et al., 1994; Miller et al., 1990; Parker et al., 1991; Powers et al., 1991, 1992, 1994a,b). This approach assumes that the rate of mass transfer is controlled by diffusional resistance in an aqueous phase boundary layer at the interface separating the two liquid phases. According to this model, the dissolution rate is the product of the film mass transfer coefficient, the interfacial area, and the concentration difference across the boundary layer. To circumvent the need for independent determination of interfacial area and film mass transfer coefficient, chemical and environmental engineers have developed dimensionless correlations representing the relationship between relevant system parameters and experimentally determined lumped mass transfer coefficients (the product of the film mass transfer coefficient and interfacial area) for a variety of porous media systems (e.g., Miller et al., 1990; Imhoff et al., 1994; Powers et al., 1994a).

Although the above modeling approaches have been successful in describing and predicting experimental soil column dissolution data (e.g., Powers et al., 1994a,b), their development and applications have been limited to water-wet systems. Porous medium wettability (the pore scale distribution of immiscible fluids near solids), however, is

actually a complex function of the solid, aqueous and organic properties. In natural soils, wettability depends on the solid phase mineralogy (Anderson, 1986), surface roughness (Morrow, 1975) and charge (Hirasaki, 1991), pH (Zheng and Powers, 1999), ionic composition (Brown and Neustadter, 1980) and strength (Murphy et al., 1992), presence of organic acids (Thomas et al., 1993) and bases (Dubey and Doe, 1993), redox condition (Wang and Guidry, 1994), and the aqueous phase film thickness (Hirasaki, 1991). In some instances, both water- and NAPL-wet solid surfaces are present in a porous medium. Such a medium is said to have fractional wettability. In the petroleum literature, fractional wettability has been recognized as an ubiquitous condition (Brown and Fatt, 1956; Donaldson et al., 1969; Salathiel, 1973). Heterogeneous distributions of water repellent soils are also a commonly reported phenomenon in the unsaturated zone (DeBano, 1969, 1981; Letey et al., 1975; Ma'sum et al., 1988; Dekker and Ritsema, 1994).

Organic liquid entrapment and two-phase flow in fractional wettability soils have been observed to be more complex than in soils that are exclusively water-wet (e.g., Morrow and Mungan, 1971; Lorenz et al., 1974; Morrow, 1976; Wang, 1988; Bradford and Leij, 1997; Bradford et al., 1999). Bradford et al. (1999) recently reported on the dissolution behavior of residual tetrachloroethylene (PCE) entrapped in a range of fractional wettability porous media. Their research reveals that an increase in the NAPL-wet soil fraction tends to result in a longer period of high effluent concentrations, followed by a more rapid rate of concentration reduction, and finally, concentration tailing at low levels. They observed a temporary effluent concentration rebound in this tailing region, following periods of flow interruption. The influence of fractional wettability on the dissolution behavior was also found to depend on the soil grain size distribution characteristics, especially for soils containing small percentages of NAPL-wet mass. These experimental observations were attributed to differences in the residual NAPL configuration, its interfacial area, and the accessibility of the residual to the flowing aqueous phase. Although consistent trends were apparent in these data, no mathematical modeling was undertaken in that work.

The objective of this paper is to explore the ability of a NAPL dissolution simulator to describe the fractional wettability dissolution data of Bradford et al. (1999). First, the mathematical framework for modeling soil column dissolution experiments is briefly reviewed. The ability of previously published dissolution correlations to predict the fractional wettability dissolution data is then examined. Next, an alternative two-parameter power function model for the lumped mass transfer coefficient is proposed and used in the simulator to fit the dissolution data. Trends in the model parameters are noted and correlation expressions are developed. Concentration tailing and rebounding behavior at large times is also explored with the simulator, using measured equilibrium sorption parameters. Finally, the simulator and fitted dissolution parameters are used to illustrate the potential influence of spatial variations in wettability on PCE dissolution behavior.

2. Mathematical modeling framework

Powers et al. (1991) presented a modeling framework to describe entrapped NAPL dissolution in one-dimensional soil columns. A slightly modified form of this develop-

ment is presented below. In soil–water–NAPL systems, a one-dimensional mass balance for a dissolved organic component in the aqueous phase can be written as:

$$\frac{\partial}{\partial t}(\theta_w C) = \frac{\partial}{\partial x} \left(\theta_w D_h \frac{\partial C}{\partial x} \right) - \frac{\partial}{\partial x}(qC) + E^{sw} + E^{ow}, \quad (1)$$

where C (ML^{-3}) is the aqueous phase organic concentration, q (LT^{-1}) is the Darcy velocity of the aqueous phase, D_h ($\text{L}^2 \text{T}^{-1}$) is the hydrodynamic dispersion coefficient, θ_w is the volumetric water content, E^{sw} ($\text{ML}^{-3} \text{T}^{-1}$) is the mass sink/source due to sorption/desorption, E^{ow} ($\text{ML}^{-3} \text{T}^{-1}$) is the source of mass due to NAPL dissolution, x (L) is vertical distance, and t (T) is time. The hydrodynamic dispersion coefficient is represented as (Bear, 1972):

$$D_h = \alpha_L \frac{q}{\theta_w} + \tau D_L, \quad (2)$$

where α_L (L) is the longitudinal dispersivity, which was approximated herein as twice the mean soil grain size (Imhoff and Miller, 1996), D_L ($\text{L}^2 \text{T}^{-1}$) is the free liquid diffusivity, and τ is the tortuosity, here set equal to $0.66\theta_w$ (Penman, 1940). Eq. (1) assumes that only the aqueous phase is mobile, and neglects surface diffusion and diffusion within the organic phase.

E^{ow} represents the exchange of mass between the organic liquid and aqueous phases and is modeled herein using a linear driving force expression (Weber and DiGiano, 1996) as:

$$E^{ow} = \frac{-\partial(\theta_o \rho_o)}{\partial t} = k_f^{ow} A^{ow} (C_s - C) = \hat{k}_1^{ow} (C_s - C) \quad (3)$$

Here, k_f^{ow} (L T^{-1}) is known as the film mass transfer coefficient, A^{ow} (L^{-1}) is the organic–water interfacial area per unit bulk volume of the medium, C_s (ML^{-3}) is the equilibrium solubility concentration which approximates the concentration at the organic–water interface, θ_o is the volumetric organic liquid content, and ρ_o (ML^{-3}) is the density of the organic liquid. Because independent determination of A^{ow} and k_f^{ow} is difficult, the lumped mass transfer coefficient ($\hat{k}_1^{ow} = A^{ow} k_f^{ow}$) (T^{-1}) will be utilized in this study.

E^{sw} represents the mass gained or lost to the aqueous phase through sorption and desorption mechanisms. Here, mass transfer limitations are hypothesized to be due to diffusional resistance in an aqueous phase boundary layer, similar to the conceptual model of dissolution (Wu and Gschwend, 1986; Ball and Roberts, 1991; Weber et al., 1991; Abriola et al., 1999). The desorption mass transfer is, thus, represented as:

$$E^{sw} = -\rho_b \frac{\partial Q}{\partial t} = k_f^{sw} A^{sw} (C_{eq}^{sw} - C) = \hat{k}_1^{sw} (C_{eq}^{sw} - C), \quad (4)$$

where ρ_b is the bulk density (ML^{-3}), k_f^{sw} (LT^{-1}) is the kinetic film sorption/desorption rate coefficient, A^{sw} (L^{-1}) is the solid–water interfacial area per unit bulk volume of medium, Q (M/M) is the sorbed phase organic concentration, and C_{eq}^{sw} (ML^{-3}) is the aqueous phase organic concentration in equilibrium with the sorbed phase organic concentration. Similar to the dissolution expression given in Eq. (3), a lumped

sorption/desorption rate coefficient ($\hat{k}_1^{\text{sw}} = A^{\text{sw}} k_f^{\text{sw}}$) (T^{-1}) will be utilized in this study. For the soil–water–NAPL systems employed in the experiments of Bradford et al. (1999), a Freundlich isotherm gave a good representation of sorption data. Thus, $C_{\text{eq}}^{\text{sw}}$ is represented as:

$$C_{\text{eq}}^{\text{sw}} = \left(\frac{Q}{K_{\text{F}}^{\text{sw}}} \right)^{\frac{1}{n}}, \quad (5)$$

where K_{F}^{sw} is the Freundlich distribution coefficient, and n (dimensionless) is the Freundlich exponent. Although the Freundlich isotherm has an empirical basis (Weber et al., 1991), theoretical analyses, such as those presented by Carter et al. (1995), suggest that K_{F}^{sw} is a measure of sorption capacity, while n characterizes the cumulative magnitude and variance of sorption energies. It should be noted that more complicated mathematical expressions have been postulated in the literature to describe sorption and desorption processes (Weber et al., 1991). Such models may incorporate more than one rate-limiting process (e.g., intra-aggregate diffusion), relax the quasi-steady assumption, or divide the domain into regions in which different mechanisms are controlling. The choice of Eq. (4) was based upon the simplicity of the model expression and the relative ease of parameter determination.

Using the above mathematical framework, a one-dimensional finite difference contaminant transport simulator, MGANGLIA, was developed for application to the soil column dissolution experiments. MGANGLIA solves Eqs. (1), (3) and (4) using a centered-difference discretization of the spatial terms and a fully implicit backward-difference discretization of the temporal terms to create a set of coupled algebraic equations that are solved sequentially using the Thomas algorithm, after implementing initial and boundary conditions. Nonlinear coefficients, including saturations and lumped mass transfer coefficients, are evaluated explicitly at the previous time level. The numerical implementation of Eqs. (1), (3) and (4) in MGANGLIA was verified by comparison of simulator output and results from one-dimensional analytical solutions and another one-dimensional NAPL dissolution simulator (GANGLIA) (Powers et al., 1994a).

3. Dissolution predictions

MGANGLIA was employed to model the dissolution experiments of Bradford et al. (1999) using known laboratory conditions and several previously reported correlations to estimate the lumped mass transfer coefficients. A complete description of the experimental protocols and procedures employed in the laboratory study is provided in the above-cited reference. In the experiments of Bradford et al. (1999), fractional wettability soils were obtained by combining various mass fractions of untreated and octadecyltrichlorosilane (OTS)-treated Ottawa sands. These soils will be designated herein by their percentage of OTS treated sands or by the equivalent NAPL-wet mass fraction (F_o). Table 1 summarizes corresponding sieve sizes and experimental conditions for 23 soil column experiments. Here, the median grain size (d_{50}) (L) and the uniformity index

Table 1
Summary of soil column properties

| Soil sieves | F_0 | θ_{10} | ε | d_{50} (cm) | U_i | q (cm/min) |
|-------------------------|-------|---------------|---------------|---------------|-------|--------------|
| <i>F20–F30</i> | | | | | | |
| | 0.00 | 0.042 | 0.327 | 0.071 | 1.210 | 0.516 |
| | 0.10 | 0.017 | 0.318 | 0.071 | 1.210 | 0.466 |
| | 0.25 | 0.018 | 0.324 | 0.071 | 1.210 | 0.481 |
| | 0.50 | 0.020 | 0.337 | 0.071 | 1.210 | 0.503 |
| | 0.75 | 0.009 | 0.342 | 0.071 | 1.210 | 0.512 |
| <i>F35–F50</i> | | | | | | |
| | 0.00 | 0.036 | 0.321 | 0.036 | 1.880 | 0.451 |
| | 0.10 | 0.031 | 0.314 | 0.036 | 1.880 | 0.480 |
| | 0.25 | 0.021 | 0.341 | 0.036 | 1.880 | 0.471 |
| | 0.50 | 0.024 | 0.341 | 0.036 | 1.880 | 0.487 |
| | 0.75 | 0.017 | 0.325 | 0.036 | 1.880 | 0.551 |
| | 1.00 | 0.021 | 0.341 | 0.036 | 1.880 | 0.470 |
| <i>F70–F110</i> | | | | | | |
| | 0.00 | 0.045 | 0.316 | 0.015 | 2.250 | 0.549 |
| | 0.10 | 0.048 | 0.326 | 0.015 | 2.250 | 0.493 |
| | 0.25 | 0.030 | 0.342 | 0.015 | 2.250 | 0.481 |
| | 0.50 | 0.034 | 0.340 | 0.015 | 2.250 | 0.455 |
| | 0.75 | 0.033 | 0.346 | 0.015 | 2.250 | 0.481 |
| | 1.00 | 0.085 | 0.348 | 0.015 | 2.250 | 0.479 |
| <i>F35–F50–F70–F110</i> | | | | | | |
| | 0.00 | 0.034 | 0.302 | 0.024 | 3.060 | 0.480 |
| | 0.10 | 0.040 | 0.301 | 0.024 | 3.060 | 0.497 |
| | 0.25 | 0.022 | 0.294 | 0.024 | 3.060 | 0.500 |
| | 0.50 | 0.015 | 0.298 | 0.024 | 3.060 | 0.520 |
| | 0.75 | 0.030 | 0.313 | 0.024 | 3.060 | 0.499 |
| | 1.00 | 0.036 | 0.306 | 0.024 | 3.060 | 0.509 |

($U_i = d_{60}/d_{10}$) are measures of the average grain size and the distribution of grain sizes, respectively; where $x\%$ of the mass is finer than d_x (L). The experimental fluids were Milli-Q water and laboratory grade (99%) PCE (Aldrich Chemical, Milwaukee, WI). PCE has a density of 1.623 g/cm³, a viscosity of 0.89 cP (Lide, 1994), an interfacial tension of 45.0 dyn/cm with water (Brown et al., 1994), an equilibrium solubility (C_s) of approximately 203 mg/l at 20°C (Bradford et al., 1999), and an aqueous phase diffusion coefficient of 6.56×10^{-6} cm²/s (Hayduk and Laudie, 1974).

Previous mass transfer correlations for soil column dissolution data have been developed assuming that the experimental porous media were “completely” water-wet. Correlations for the lumped mass transfer coefficient in these studies have frequently been expressed as power functions of dimensionless variables. The mass transfer coefficient is typically incorporated in these correlations through a dimensionless modified Sherwood number ($Sh^{ow} = \hat{k}_1^{ow}(d_{50})^2/D_L$). Other dimensionless variables include the Reynolds ($Re = \rho_w v_w d_{50}/\mu_w$; v_w (L T⁻¹) is the pore water velocity, and ρ_w (ML⁻³) and μ_w (ML⁻¹ T⁻¹) are the aqueous phase density and viscosity,

respectively) and Schmidt ($Sc = \mu_w / (\rho_w D_L)$) numbers. Mass transfer correlations that have appeared in the literature to describe the complete dissolution of residual organic liquids from sandy media include that of Powers et al. (1994a):

$$Sh^{ow} = 4.13 Re^{0.598} \delta^{0.673} U_i^{0.369} \left(\frac{\theta_o}{\theta_{io}} \right)^{0.518 + 0.114\delta + 0.10U_i} \quad (6)$$

Imhoff et al. (1994):

$$Sh^{ow} = 340 Re^{0.71} \theta_o^{0.87} \left(\frac{X}{d_{50}} \right)^{-0.31} \quad (7)$$

and Imhoff et al. (1997):

$$Sh^{ow} = 1.34 Re^{0.75} Sc^{0.486} \theta_o^{0.9} \quad (8)$$

Here, the symbol δ represents a dimensionless mean grain size ($\delta = d_{50}/d_M$, where $d_M = 0.05$ cm), θ_{io} is the initial volumetric organic liquid content, and X denotes the distance from the column inlet. (In accordance with Imhoff et al. (1994), upper and lower limits for X were set equal to $1.4d_{50}$ and $180d_{50}$, respectively.) Imhoff and Miller (1996) reported that the parameter X/d_{50} in Eq. (7) was used to capture the effects of dissolution fingering. If dissolution fingering does not occur, Imhoff and Miller (1996) suggested that X/d_{50} be set equal to 7. In this work, the more general correlation (Eq. 7) is employed.

Fig. 1a–d presents comparisons of model predictions, using the correlations in Eqs. (6)–(8), with measured effluent concentrations (Bradford et al., 1999) for the completely water-wet F20–F30, F35–F50, F35–F50–F70–F110 and F70–F110 sand systems, respectively. The log of C/C_s is plotted as a function of pore volumes (product of the porosity and column volume) of water that have passed through the column. For comparison purposes, the equilibrium prediction (no dissolution mass transfer limitations) is also presented. Note that for all systems, the equilibrium prediction significantly underestimates the remediation time. Furthermore, observe that no single correlation provides a good description of all the water-wet dissolution data sets. The correlations of Powers et al. (1994a) (Eq. 6), Imhoff et al. (1994) (Eq. 7) and Imhoff et al. (1997) (Eq. 8) provide the best predictions of the F20–F30 (Fig. 1a), F35–F50 (Fig. 1b) and F35–F50–F70–F110 (Fig. 1c) data sets, respectively. None of the above correlations was able to accurately predict the dissolution behavior of PCE entrapped in the F70–F110 sand (cf. Fig. 1d). One possible explanation for these observations is obtained by considering the ranges in mean grain sizes that were employed in the development of each correlation. The experimental range for d_{50} was 0.045–0.12 cm for Powers et al. (1994a) (Eq. 6), and 0.03–0.042 cm for Imhoff et al. (1994) (Eq. 7). The correlation of Imhoff et al. (1997) (Eq. 8) was developed for a single sand ($d_{50} = 0.028$ cm). Comparison of the d_{50} values of the sands employed in Fig. 1 (cf. Table 1) with the d_{50} ranges of the correlations reveals that the best prediction was obtained with a particular correlation when the d_{50} value of the soil was most consistent with that used in correlation development. This result suggests that the above correlations are strictly valid only for the parameter ranges under which they were developed, and that caution

should be exercised when applying such correlations to systems, which fall outside these ranges.

All of the correlations previously developed for NAPL dissolution are independent of soil wettability conditions. An assumption of water-wet conditions, however, is implicit in their development. As an example of the potential magnitude of the prediction error that will occur if this assumption is violated, consider the fractional wettability dissolu-

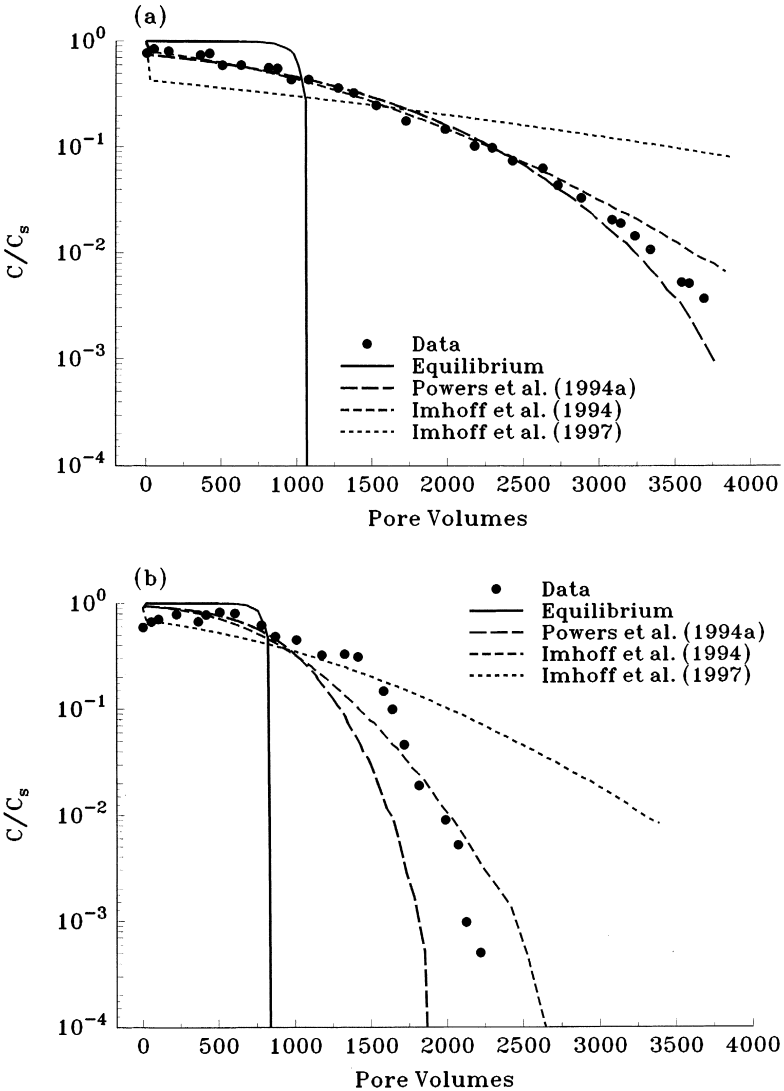


Fig. 1. Observed and predicted effluent concentration curves for the completely water-wet F20–F30 (a), F35–F50 (b), F35–F50–F70–F110 (c), and F70–F110 (d) sand systems. The predictions were obtained from previously published mass transfer correlations (Eqs. 6–8).

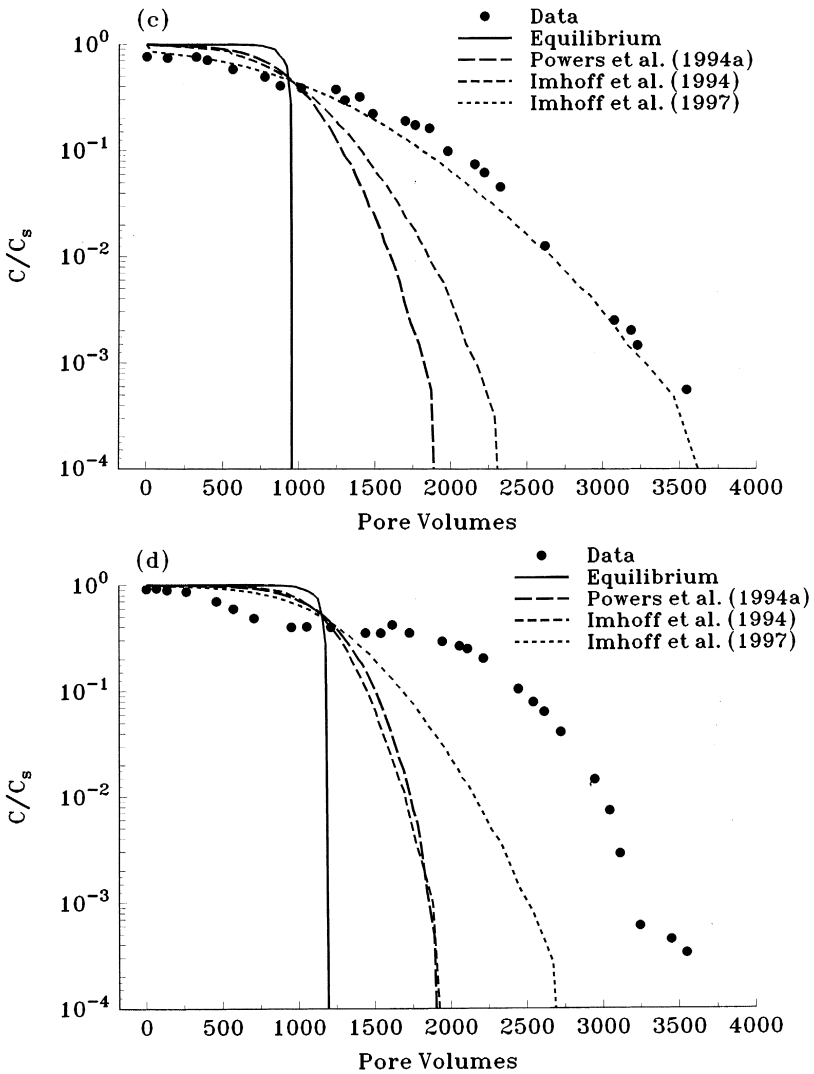


Fig. 1 (continued).

tion data for the F35–F50–F70–F110 sand shown in Fig. 2. Here, to highlight the influence of wettability, normalized concentration curves have been “shifted” along the abscissa, so that the area under each curve represents the same mass of organic. This mass is equivalent to a volumetric organic content of 0.02. After this shifting operation, the volume of water that is passed through the column is referred to as a “shifted volume” (V'). Inspection of Fig. 2 reveals that very significant differences in dissolution behavior occur as a result of variations in wettability. Consequently, correlations that adequately predict the dissolution time of the water-wet F35–F50–F70–F110 soil will significantly overestimate the dissolution time for the fractional wettability systems.

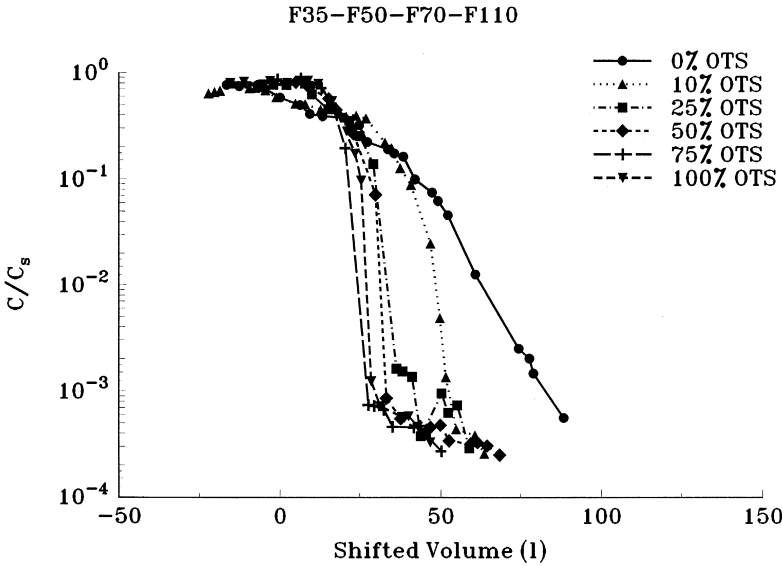


Fig. 2. The various fractional wettability dissolution data for the F35–F50–F70–F110 sand. Here, a log plot of C/C_s as function of shifted volumes (V') is presented. Reproduced from Bradford et al. (1999), copyright by the American Geophysical Union.

It is obvious from Figs. 1 and 2 that none of the above correlations, Eqs. (6)–(8), will provide an adequate description of the fractional wettability dissolution data shown in Fig. 2.

4. Fractional wettability correlation development

Due to the inability of the above correlations to predict the fractional wettability dissolution behavior, a more general mass transfer function was sought. A common feature of the mass transfer correlations given in Eqs. (6)–(8) is that they employ a simple volumetric NAPL content power function as a surrogate parameter for temporal changes in interfacial area. They all exhibit a similar power function dependence on the Reynolds number. Only Eq. (8) includes a dependence on the Schmidt number. A number of studies that have considered the initial dissolution behavior of organic liquids, however, have found a similar dependence on the Schmidt number (cf. Miller et al., 1990). The mass transfer correlation was therefore assumed to have the following functional form:

$$Sh^{ow} = \alpha Re^{0.654} Sc^{0.486} \left(\frac{\theta_o}{\theta_{io}} \right)^\beta \tag{9}$$

Here, α and β are fitting parameters. In this correlation, the value of α will control the initial ($\theta_o \approx \theta_{io}$) dissolution behavior, whereas β will influence the long-term transient

dissolution behavior. The value of β is assumed to range between zero and one. Note that the magnitude of Sh^{ow} and, hence, \hat{k}_1^{ow} , is less sensitive to changes in NAPL content as β decreases. The value of the exponent on the Reynolds number given in Eq. (9) was chosen to have an intermediate value to those given in Eqs. (6)–(8). This value was taken from the mass transfer correlation of Powers et al. (1994b) that was established from soil column dissolution measurements of solid naphthalene spheres, with a known interfacial area, that were emplaced in sandy porous media.

The ability of Eq. (9) to describe the fractional wettability dissolution data was investigated by fitting the parameters α and β to column effluent data. The value of E^{sw} (cf. Eq. 1) was set equal to zero ($K_F^{sw} = 0$) during this fitting procedure and, hence, this approach, cannot capture the low concentration tailing behavior ($C/C_s < 0.001$) observed in Fig. 2. Fitting was achieved by incorporating MGANGLIA into an optimization program based on the Levenberg–Marquardt algorithm (Levenberg, 1944; Marquardt, 1963). This algorithm combines a quadratic-extrapolation strategy with a steepest descent approach to minimize the sum of the squared error between observed and predicted concentrations (the objective function). The fitting routine is strongly dependent on the initial parameter estimates. To reduce non-uniqueness problems, the value of α was fitted to the dissolution dataset for a particular soil that exhibited the least sensitivity to β ($\beta \approx 0$), i.e., the most NAPL-wet sand system (75% or 100% OTS). This value of α was then held constant for the other fractional wettability soils of that size fraction, while the value of β was fitted. This fitting approach implicitly assumes that β can account for the influence of soil wettability on dissolution and that α is primarily determined by system hydrodynamics. The choice of the objective function will also influence the fitting results. Since a wide variety of dissolution behaviors occurred in the datasets and concentrations ranged over four orders of magnitude, two objective functions were considered: the normalized objective function (the difference in the observed and predicted concentrations was normalized by the magnitude of the observed concentration) that gives equal weight to each observed data point (concentration) and the unnormalized objective function, that gives less weight to lower concentration values. In general, the normalized objective function was employed to fit systems, which exhibited more gradual changes in effluent concentrations (e.g., lower OTS systems).

Table 2 summarizes best fit values of the dissolution model parameters (α and β), as well as statistical parameters for the goodness of fit (e.g., Myers, 1986; Samuels, 1989); i.e., the coefficient of linear regression (r^2), the mean square error (MSE) and the 95% confidence interval on fitted parameters determined according to the Student's t test. Examples that best fit to several observed dissolution datasets are presented in Fig. 3. Observe in Fig. 3a and b that good fits are achieved with Eq. (9) for the water-wet and NAPL-wet dissolution data, respectively. This observation suggests that the proposed functional form for the mass transfer coefficient can accurately capture the dissolution behavior of residual NAPL whether entrapped as ganglia or films. Poorer model fits were sometimes obtained for the lower NAPL-wet sand fraction systems. This observation is believed to be related to the increased sensitivity of the effluent concentrations to the presence of persistent large ganglia (lower interfacial area to NAPL volume) in these systems (e.g., Imhoff et al., 1998). Fig. 3c shows the observed and best fit effluent

Table 2
Fitted dissolution parameters

| F_0 | α | β | r^2 | MSE | 95% Confidence interval |
|-------------------------|----------|---------|-------|-------|--------------------------------|
| <i>F20–F30</i> | | | | | |
| 0.00 | 0.239 | 1.000 | 0.987 | 0.001 | $0.973 \leq \beta \leq 1.000$ |
| 0.10 | 0.239 | 0.555 | 0.599 | 0.034 | $0.000 \leq \beta \leq 1.000$ |
| 0.25 | 0.239 | 0.031 | 0.984 | 0.003 | $0.000 \leq \beta \leq 0.164$ |
| 0.50 | 0.239 | 0.039 | 0.980 | 0.003 | $0.000 \leq \beta \leq 0.190$ |
| 0.75 | 0.239 | 0.000 | 0.996 | 0.001 | $0.219 \leq \alpha \leq 0.259$ |
| <i>F35–F50</i> | | | | | |
| 0.00 | 0.103 | 0.826 | 0.850 | 0.015 | $0.820 \leq \beta \leq 0.833$ |
| 0.10 | 0.103 | 0.780 | 0.860 | 0.017 | $0.730 \leq \beta \leq 0.830$ |
| 0.25 | 0.103 | 0.297 | 0.981 | 0.003 | $0.268 \leq \beta \leq 0.327$ |
| 0.50 | 0.103 | 0.001 | 0.986 | 0.002 | $0.000 \leq \beta \leq 0.181$ |
| 0.75 | 0.103 | 0.059 | 0.993 | 0.001 | $0.058 \leq \beta \leq 0.061$ |
| 1.00 | 0.103 | 0.000 | 0.977 | 0.003 | $0.087 \leq \alpha \leq 0.120$ |
| <i>F70–F110</i> | | | | | |
| 0.00 | 0.054 | 1.000 | 0.760 | 0.022 | $0.988 \leq \beta \leq 1.000$ |
| 0.10 | 0.054 | 0.982 | 0.918 | 0.009 | $0.901 \leq \beta \leq 1.000$ |
| 0.25 | 0.054 | 0.203 | 0.979 | 0.003 | $0.182 \leq \beta \leq 0.223$ |
| 0.50 | 0.054 | 0.001 | 0.968 | 0.005 | $0.000 \leq \beta \leq 0.163$ |
| 0.75 | 0.054 | 0.003 | 0.976 | 0.004 | $0.000 \leq \beta \leq 0.146$ |
| 1.00 | 0.054 | 0.000 | 0.929 | 0.010 | $0.047 \leq \alpha \leq 0.062$ |
| <i>F35–F50–F70–F110</i> | | | | | |
| 0.00 | 0.047 | 0.901 | 0.972 | 0.002 | $0.897 \leq \beta \leq 0.913$ |
| 0.10 | 0.047 | 0.647 | 0.890 | 0.008 | $0.632 \leq \beta \leq 0.663$ |
| 0.25 | 0.047 | 0.606 | 0.982 | 0.002 | $0.557 \leq \beta \leq 0.655$ |
| 0.50 | 0.047 | 0.645 | 0.995 | 0.000 | $0.629 \leq \beta \leq 0.661$ |
| 0.75 | 0.047 | 0.060 | 0.973 | 0.004 | $0.055 \leq \beta \leq 0.065$ |
| 1.00 | 0.047 | 0.000 | 0.978 | 0.003 | $0.042 \leq \alpha \leq 0.052$ |

concentration curves for F70–F110 10% OTS and F35–F50 25% OTS soils. Note that the experimental dissolution curves appear to exhibit an inflection point. The initial dissolution behavior is believed to be controlled by higher interfacial area per NAPL volume organic films. Once these films dissolve, an inflection point occurs in the effluent concentration curve when the larger ganglia start to control the dissolution behavior. The inflection point occurs around 1700 and 800 pore volumes for the F70–F110 10% OTS and F35–F50 25% OTS systems, respectively. The proposed model for the lumped mass transfer coefficient (Eq. 9) cannot capture this inflection point. To achieve a better fit to these data, a considerably more complex correlation expression, incorporating terms for both organic ganglia distributions and films, would likely be required.

Inspection of Table 2 reveals that the value of α tends to decrease with decreasing mean grain size and increasing uniformity coefficient. A correlation between the fitted values of α and these grain size distribution characteristics was sought to facilitate the prediction of the fractional wettability dissolution data. The previously discussed

nonlinear least squares fitting routine was utilized for this purpose. The value of α was found to depend on δ and U_i as:

$$\alpha = 0.254\delta^{0.475}U_i^{-1.187}; \quad r^2 = 0.999. \quad (10)$$

The 95% confidence interval for the exponents on δ and U_i were determined to be from 0.134 to 0.816, and from -1.77 to -0.604 , respectively, while that for the lead coefficient in Eq. (10) was from 0.194 to 0.313.

Fig. 4 presents a plot of the variation of fitted values of β with F_o for the various soils. Observe in Table 2 and Fig. 4 that the value of β depends strongly on the NAPL-wet mass fraction (the wettability), decreasing with increasing F_o . This observation suggests a decreased sensitivity to changes in NAPL saturation as the NAPL-wet fraction increases; i.e., NAPL films maintain high interfacial areas (effluent concentrations) until they completely dissolve. Note in Fig. 4 that the value of β also depends on the grain size distribution characteristics. The most graded soil exhibits a much more gradual decrease in β with increasing F_o than the more uniform soils. One possible explanation is due to a decrease in accessibility of the NAPL to flowing water as the soil gradation increases (Bradford et al., 1999). Similar to α , a correlation between β and experimental parameters was therefore sought to facilitate the prediction of the fractional wettability dissolution data. The nonlinear least squares fitting routine was again utilized for this purpose. In this case, the value of β was found to depend on F_o and U_i as:

$$\beta = 0.959(1.0 - F_o)^{\frac{6.265}{U_i}}; \quad r^2 = 0.879. \quad (11)$$

The 95% confidence interval for the exponent on $(1 - F_o)$ was from $4.015/U_i$ to $8.515/U_i$, while that for the lead coefficient in Eq. (11) was from 0.827 to 1.09. The above correlation provides a reasonable description of fitted β values for the uniform soils (F20–F30, F35–F50 and F70–F110), but tends to significantly under predict β values at intermediate OTS values for the most graded soil (F35–F50–F70–F110).

The correlations for α (Eq. 10) and β (Eq. 11) can be incorporated into Eq. (9) to facilitate comparison with the previous mass transfer correlations (Eqs. 6–8). Note that Eqs. (10) and (6) show a dependence on the soil grain size distribution parameters δ and U_i . In contrast, grain size distribution parameters were not significantly varied in the studies of Imhoff et al. (1994, 1997) and, hence, Eqs. (7) and (8), do not show a dependence on these parameters. Comparison of Eqs. (6) and (10) reveals a similar dependence on δ (exponents within the 95% confidence interval 0.134–0.816). In contrast, the dependence of Sh^{ow} on U_i in these two correlations is strikingly different. In Eq. (6), a positive dependence was found, whereas in this work (cf. Eq. 10), an inverse dependence was observed. This discrepancy is likely a result of differences in porous media wettability in these studies; i.e., Eq. (10) is based on long-term dissolution data for residual PCE entrapped in PCE-wet soils, whereas Eq. (6) was developed from initial dissolution rates for NAPLs entrapped in water-wet soils. A direct comparison of β values in Eqs. (6)–(8) and (11) is only possible for the water-wet case. In this work, the fitted values of β for water-wet soils ranged from 0.826 to 1.00 (cf. Table 2); Eq. (11) predicts a mean value of β equal to 0.959. The predicted β values for these soils

according to Eqs. (6)–(8) are similar in magnitude, but tend to be a little lower (falling within the range 0.78–0.9) than those found in this study.

To investigate the utility and limitations of the above correlations in capturing the observed column dissolution behavior, the fractional wettability dissolution experiments (cf. Table 1) were modeled using MGANGLIA in conjunction with Eqs. (9)–(11). Fig.

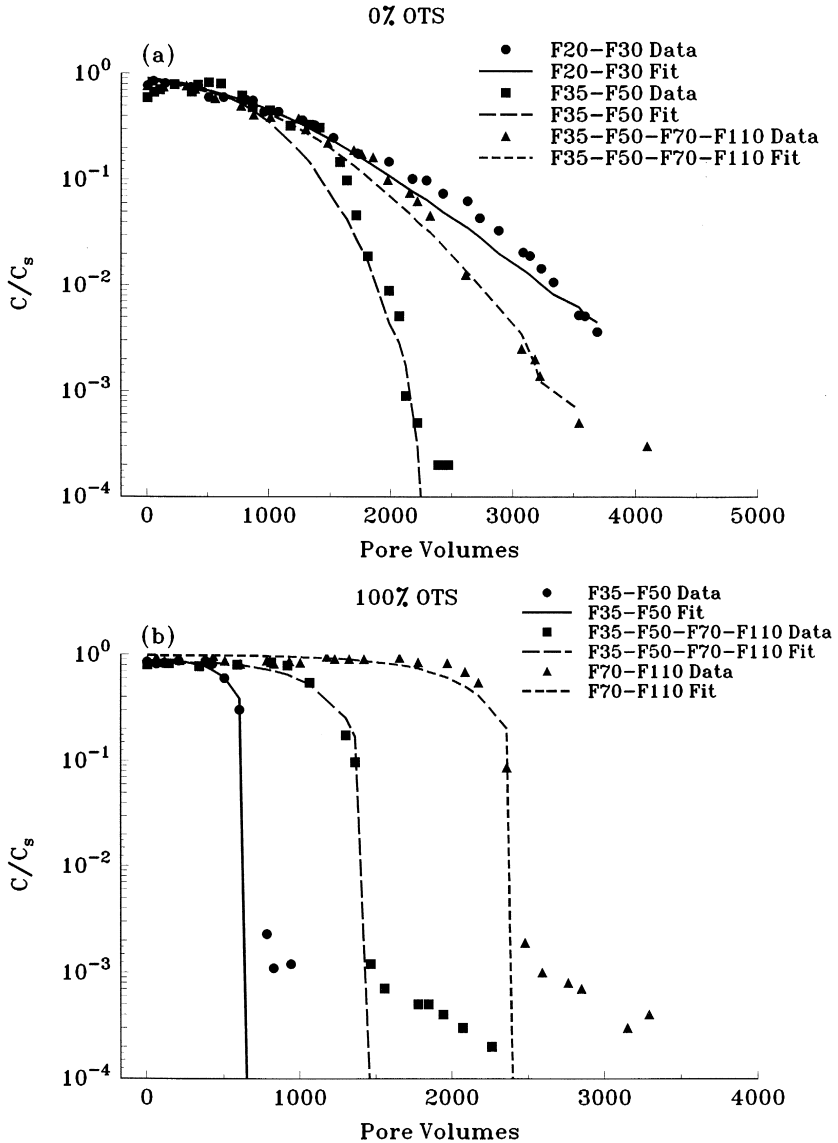


Fig. 3. Observed and best fit (Eq. 9) effluent concentration curves for water-wet (a) and NAPL-wet (b) data. (c) Presents similar data for F70–F110 10% OTS and F35–F50 25% OTS systems.

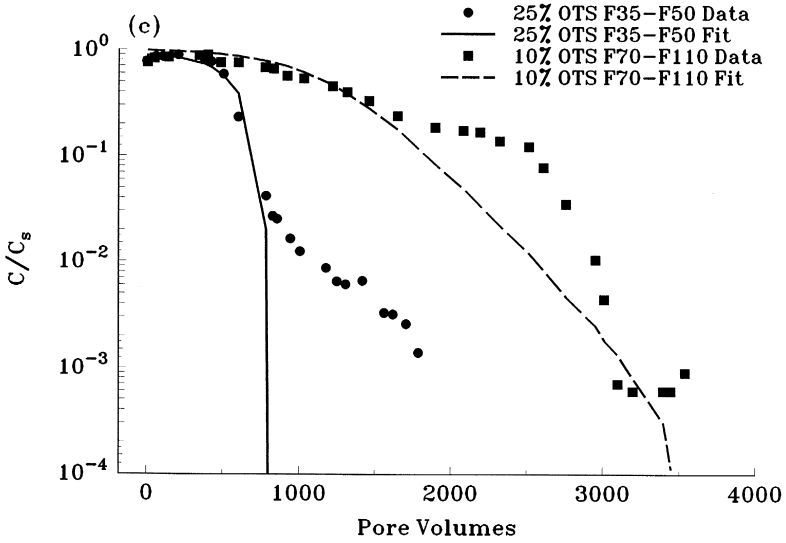


Fig. 3 (continued).

5a,b,c presents the observed and modeled effluent concentration curves for PCE entrapped in the same soils presented in Fig. 3. Note in Fig. 5a and b that the agreement between observed and predicted data is somewhat poorer for the water-wet systems (Fig. 5a) than the completely NAPL-wet systems (Fig. 5b). This observation can be attributed to the increased sensitivity of effluent concentration curves to β at higher values. Variation of β within its range of uncertainty has a greater influence on the predicted remediation time when β is larger (lower OTS systems; Imhoff et al., 1998). The

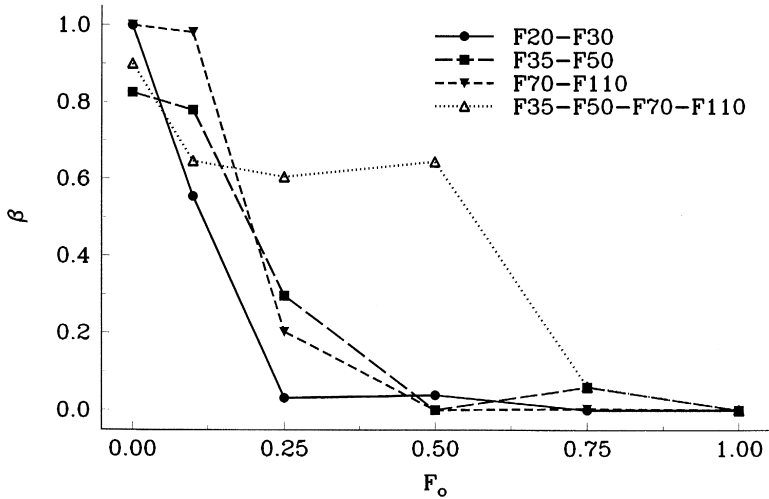


Fig. 4. A plot of the fitted values of β as a function of F_o for the various soils.

predictions for dissolution data from the 0% OTS F35–F50 (Fig. 5a) and F70–F110 soils, and for 10% OTS F70–F110 (Fig. 5c) and F35–F50–F70–F110 soils were especially poor. Comparison of Figs. 1 and 5 reveals, however, that application of Eqs.

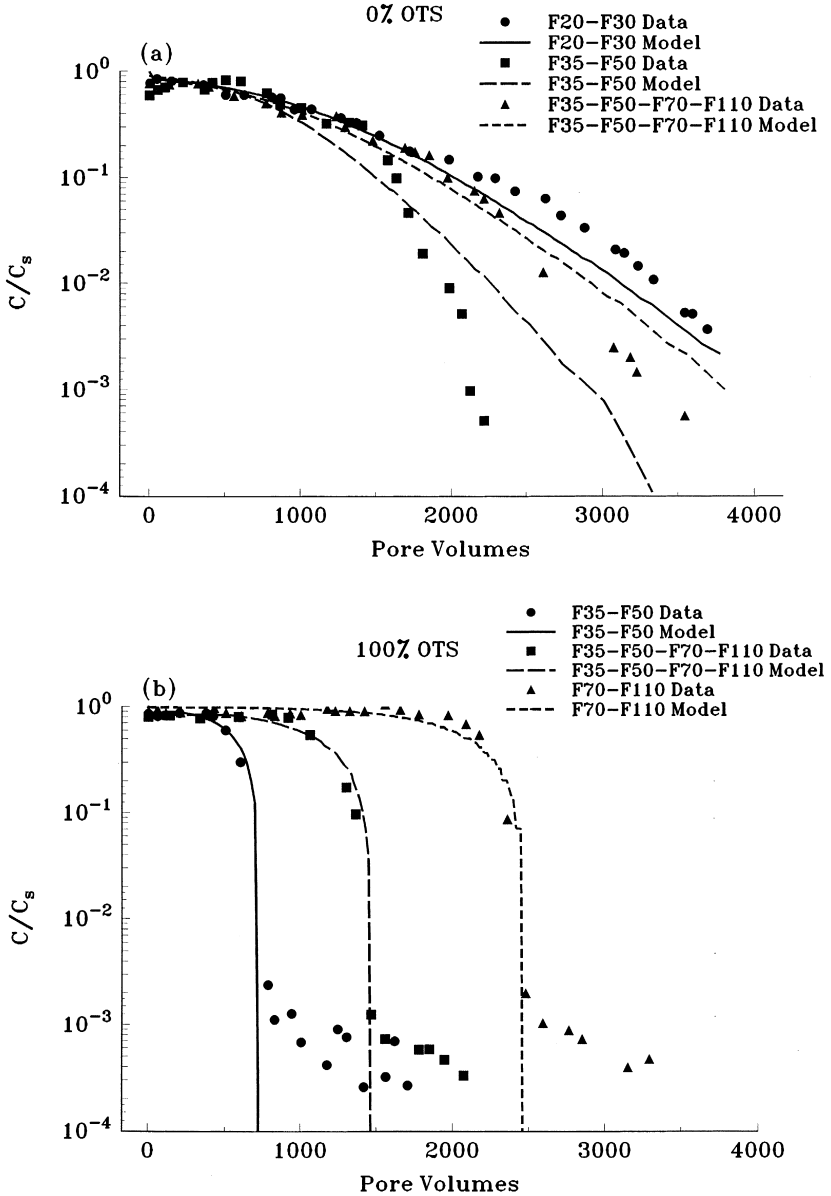


Fig. 5. Observed and predicted effluent concentration curves for PCE entrapped in several 0% (a) and 100% (b) OTS systems. (c) Presents similar data for F70–F110 10% OTS and F35–F50 25% OTS systems.

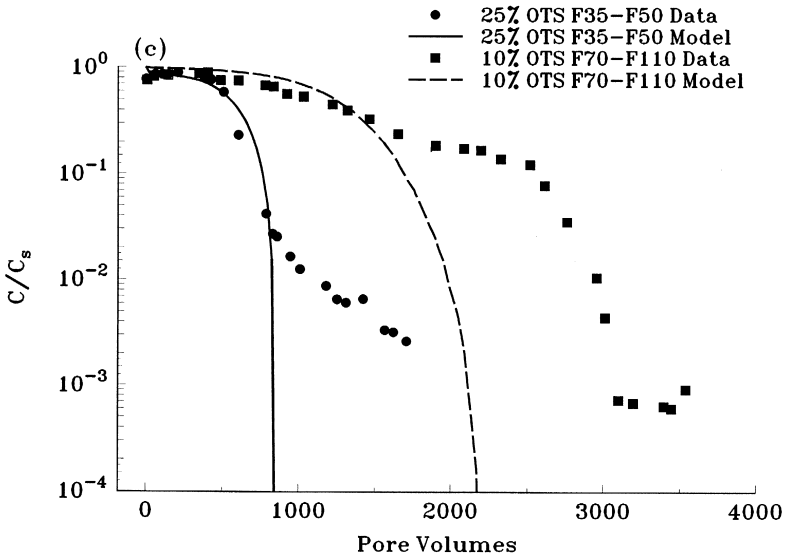


Fig. 5 (continued).

(9)–(11) generally produced a better match to the water-wet data than application of Eqs. (6)–(8).

5. Modeling long-term concentration tailing

The above discussion has focused on the effluent concentration behavior for C/C_s greater than 0.001. This section explores the long tailing at low concentration levels ($C/C_s < 0.001$) observed in the fractional wettability dissolution experiments (cf. Figs. 2 and 3b); such tailing was not observed for PCE entrapped in water-wet porous media. Bradford et al. (1999) hypothesized that tailing behavior in fractional wettability systems was due to desorption of PCE from the OTS-treated sands and/or to slow dissolution from low interfacial area or inaccessible ganglia or films. Flow interruption techniques were employed to assess the presence of separate phase PCE in these columns during tailing. Theoretically, if separate phase PCE is still present in a column, the effluent concentration should rebound to near equilibrium solubility levels when flow is reinitiated, provided that the flow interruption occurs for a sufficient duration (Pennell et al., 1993). Analysis of the concentration rebound behavior following a flow interruption (Bradford et al., 1999) suggested that small volumes of separate phase PCE (low interfacial area ganglia) may have been present in some of the lower OTS soils; the concentration rebound, however, was always less than 16% of C_s . The concentration tailing and rebound behavior for the higher NAPL-wet fraction systems were not consistent with the presence of separate phase PCE. Mathematical modeling is used below, in conjunction with equilibrium sorption measurements, to explore the hypothesis

that rate-limited PCE desorption from the OTS-treated sands is responsible for the observed low concentration tailing.

To quantify the equilibrium sorptive capacity of the experimental systems, a series of batch isotherm experiments was conducted for the 100% OTS treated sands. Sorption experiments were performed in 30-ml glass centrifuge tubes (Corex) with PTFE-faced silicone septa and caps. A 15-g sample of dry OTS coated Ottawa sand was added to the centrifuge tubes. The aqueous phase for these experiments was a mixture of 0.01 M CaCl_2 solution in de-aired Milli-Q water and an appropriate amount of stock contaminant solution. The stock contaminant solution was prepared by dissolving a known mass of PCE in methanol. Initial aqueous phase solution concentrations ranged from 0.1 to 150 ppm PCE. The centrifuge tubes were completely filled with the aqueous phase and immediately capped to minimize volatile losses. Centrifuge tubes were continuously shaken in a temperature-controlled room (25°C). In order to determine the appropriate adsorption equilibration time for mixing, kinetic batch studies were performed simultaneously for each soil type and the highest aqueous phase concentration. Triplicate samples were analyzed for a period of 30 days. After 7 days, no significant change in aqueous phase concentration was observed. Supernatant aqueous phase concentration was determined using a Hewlett-Packard Gas Chromatograph equipped with an electron capture detector (ECD). Sorbed contaminant mass was determined from differences in initial and supernatant aqueous phase concentrations.

The equilibrium sorption data for the OTS sands conformed to a Freundlich type isotherm (cf. Eq. 5). The batch-fitted parameters for each of the sands are presented in Table 3. If the OTS is primarily a surface coating, then the value of K_F^{sw} is theoretically related to the surface area of the sands. Assuming that the sands have the same degree of surface roughness, this implies that K_F^{sw} should increase with decreasing d_{50} . Table 3 indicates that the F20–F30 soil does not follow this trend. The F20–F30 sand was purchased from Fisher Scientific, whereas the other sands were obtained from US Silica. One possible explanation for the observed trend in K_F^{sw} is that the F20–F30 sand has a greater surface roughness than the US Silica sands. Surface roughness can lead to differences in surface area of several orders of magnitude (Anbeek, 1993). Surface roughness was not further investigated herein since this information was not deemed critical to this study. Since the sorption capacity of the untreated sand was confirmed to be negligible compared to the OTS treated sand, the equilibrium sorption capacity of organosilane-coated and uncoated sand mixtures was estimated as the product of the K_F^{sw} measured for that organosilane-coated sand (cf. Table 3) and F_o .

Table 3
Freundlich sorption parameters

| Soil sieves | K_F^{sw} | n |
|------------------|-------------------|------|
| F20–F30 | 2.01 | 1.06 |
| F35–F50 | 1.50 | 1.04 |
| F35–F50–F70–F110 | 1.75 | 0.98 |
| F70–F110 | 2.23 | 0.86 |

Note that the above parameters will yield Q in units of μg of PCE/g soil when $C_{\text{eq}}^{\text{sw}}$ is in units of mg/l.

Theoretically (cf. Eq. 4) the value of \hat{k}_1^{sw} could be a function of saturation due to temporal changes in A^{sw} during dissolution (organic films can dissolve from the NAPL-wet solid surfaces, exposing these surfaces to water). A constant value of \hat{k}_1^{sw} was assumed herein since the magnitude of E^{sw} does not significantly influence the aqueous phase concentration until all of the separate phase PCE is recovered (i.e., when $E^{ow} \approx 0$ and A^{sw} is constant). MGANGLIA was used in conjunction with the nonlinear least squares fitting program and the fractional wettability dissolution datasets to develop estimates of the sorption/desorption rate coefficient \hat{k}_1^{sw} (cf. Eq. 4). The previously fitted values of α and β (cf. Eq. 9 and Table 2) were held constant and the equilibrium values of C_{eq}^{sw} were determined from the equilibrium sorption parameters (Table 3).

Table 4 presents the fitted values of \hat{k}_1^{sw} , as well as statistical parameters associated with the goodness of fit (r^2 , MSE) and the 95% confidence intervals. Note that the values of \hat{k}_1^{sw} are relatively insensitive to the mass fraction of OTS-treated sands in the different soils. This result is consistent with a desorption process, which is controlled by

Table 4
Fitted lumped sorption/desorption mass transfer coefficients

| F_o | \hat{k}_1^{sw} (1/day) | r^2 | MSE | 95% Confidence interval |
|-------------------------|--------------------------|-------|-------|--|
| <i>F20–F30</i> | | | | |
| 0.10 | 0.063 | 0.769 | 0.023 | $0.000 \leq \hat{k}_1^{sw} \leq 0.181$ |
| 0.25 | 0.055 | 0.982 | 0.003 | $0.013 \leq \hat{k}_1^{sw} \leq 0.098$ |
| 0.50 | 0.052 | 0.979 | 0.003 | $0.017 \leq \hat{k}_1^{sw} \leq 0.086$ |
| 0.75 | 0.026 | 0.995 | 0.001 | $0.003 \leq \hat{k}_1^{sw} \leq 0.050$ |
| <i>F35–F50</i> | | | | |
| 0.10 | 0.000 | 0.859 | 0.017 | $0.000 \leq \hat{k}_1^{sw} \leq 0.524$ |
| 0.25 | 0.152 | 0.981 | 0.003 | $0.000 \leq \hat{k}_1^{sw} \leq 2.289$ |
| 0.50 | 0.170 | 0.984 | 0.002 | $0.000 \leq \hat{k}_1^{sw} \leq 2.405$ |
| 0.75 | 0.079 | 0.994 | 0.001 | $0.066 \leq \hat{k}_1^{sw} \leq 0.092$ |
| 1.00 | 0.085 | 0.988 | 0.002 | $0.041 \leq \hat{k}_1^{sw} \leq 0.130$ |
| <i>F70–F110</i> | | | | |
| 0.10 | 0.027 | 0.917 | 0.009 | $0.000 \leq \hat{k}_1^{sw} \leq 0.093$ |
| 0.25 | 0.071 | 0.978 | 0.003 | $0.040 \leq \hat{k}_1^{sw} \leq 0.102$ |
| 0.50 | 0.063 | 0.956 | 0.007 | $0.044 \leq \hat{k}_1^{sw} \leq 0.083$ |
| 0.75 | 0.022 | 0.954 | 0.007 | $0.011 \leq \hat{k}_1^{sw} \leq 0.032$ |
| 1.00 | 0.068 | 0.917 | 0.012 | $0.048 \leq \hat{k}_1^{sw} \leq 0.088$ |
| <i>F35–F50–F70–F110</i> | | | | |
| 0.10 | 0.099 | 0.890 | 0.009 | $0.000 \leq \hat{k}_1^{sw} \leq 1.106$ |
| 0.25 | 0.070 | 0.982 | 0.002 | $0.028 \leq \hat{k}_1^{sw} \leq 0.112$ |
| 0.50 | 0.061 | 0.995 | 0.000 | $0.048 \leq \hat{k}_1^{sw} \leq 0.074$ |
| 0.75 | 0.049 | 0.974 | 0.004 | $0.035 \leq \hat{k}_1^{sw} \leq 0.063$ |
| 1.00 | 0.054 | 0.977 | 0.004 | $0.036 \leq \hat{k}_1^{sw} \leq 0.072$ |

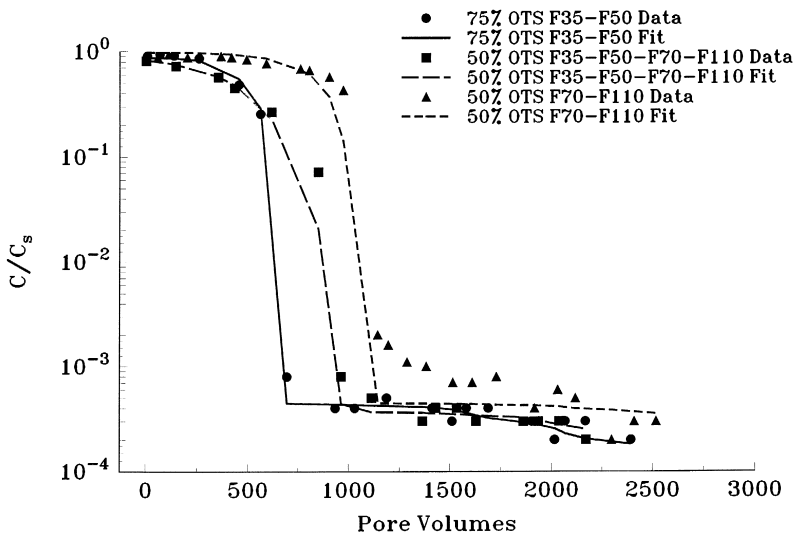


Fig. 6. A plot of the observed and fitted effluent concentration curves, including concentration tailing, for the indicated fractional wettability dissolution datasets.

system hydrodynamics, as would be anticipated if sorption is occurring as partitioning to surface coatings. Note that high values of \hat{k}_1^{sw} occur for the 25% and 50% OTS F35–F50 sands. These values are believed to be nonphysical and a consequence of the inability of the dissolution model to capture the observed trends in effluent concentration data (cf. Fig. 3c) for these systems.

Fig. 6 provides a plot of the observed and fitted effluent concentration curves, including concentration tailing, for several fractional wettability dissolution datasets. Note that the use of measured equilibrium sorption data in conjunction with the fitted values of \hat{k}_1^{sw} provides a reasonable representation of the low concentration data. Lamarche (1991) observed similar low concentration tailing behavior in dissolution experiments. Recently, Miller et al. (1998) suggested that this concentration tailing behavior could be due to dissolution fingering. However, the potential for sorption was not evaluated. The above analysis suggests that, for the experiments analyzed herein, rate-limited desorption provides a reasonable explanation for this behavior.

6. Applications

Spatial variations in wettability will occur in the field as a result of natural processes (e.g., mineralogy, organic matter, redox conditions, aqueous phase chemistry, etc.) or remediation activities (e.g., injection of surfactants or strong oxidizers). One-dimensional numerical experiments were conducted with MGANGLIA to explore the potential influence of spatial variations in wettability properties on PCE dissolution behavior at the column scale. These simulations used the fitted dissolution parameters (α and β)

presented in Table 2. Here, the emphasis was on NAPL dissolution; sorption was neglected. The modeled domain was a 5-cm long vertical soil column packed with sand (cf. Table 1) to a porosity of 0.33. PCE was initially entrapped at a uniform saturation of 7.5%. For a given soil grain size distribution and column averaged fractional wettability, three packing configurations were considered: (i) a uniform distribution of fractional wettability; (ii) a two-layer distribution with NAPL-wet and water-wet layers at the column inlet and outlet, respectively; and (iii) a two-layer distribution with these layers reversed. Distributions (i), (ii), and (iii) will be referred to below as “OTS-uniform”, “OTS-inlet”, and “OTS-outlet”, respectively. Column-averaged fractional wettabilities of 10%, 25%, 50% and 75% OTS sands were considered for each soil grain size distribution (cf. Table 1). The “complete” dissolution of the residual PCE was then simulated for water flowing upward through the column at a constant Darcy velocity of 0.45 cm/min.

Fig. 7 presents illustrative effluent concentration curves for the 50% OTS (column averaged) F35–F50 soil for various distributions of wettability. The time (pore volumes) required to achieve an effluent concentration four orders of magnitude below the equilibrium solubility is significantly influenced by the spatial distribution of wettability. This remediation time was greatest for the OTS-inlet distribution and shortest for the OTS-uniform distribution. Note also that the shape of the effluent concentration curves depends strongly on the wettability distribution. The OTS-inlet and OTS-outlet distributions resulted in inflection points in the effluent concentration curves at 570 and 845 pore volumes, respectively. The change in the effluent concentration at the inflection point is much more pronounced for the OTS-outlet condition than for the OTS-inlet condition.

Many of the soil–water–PCE systems exhibited similar dissolution behavior to that shown in Fig. 7. Fig. 8 summarizes the simulated remediation times for the various

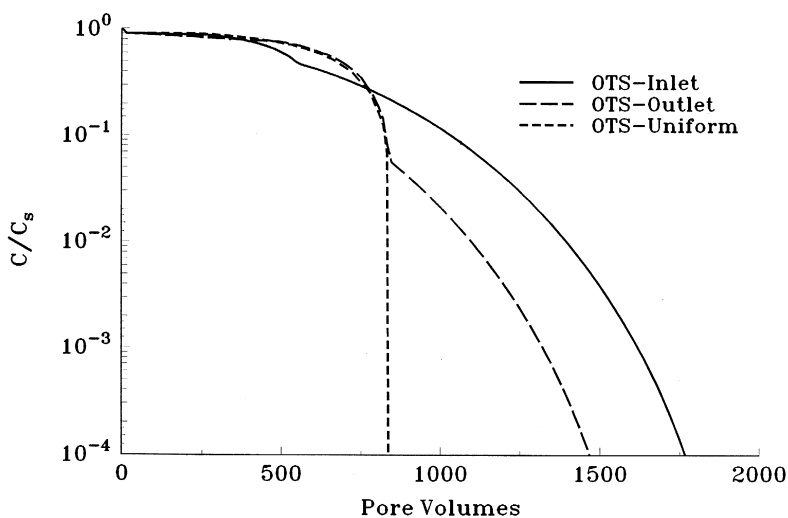


Fig. 7. Illustrative effluent concentration curves for the 50% OTS (column-averaged) F35–F50 soil for various distributions of wettability.

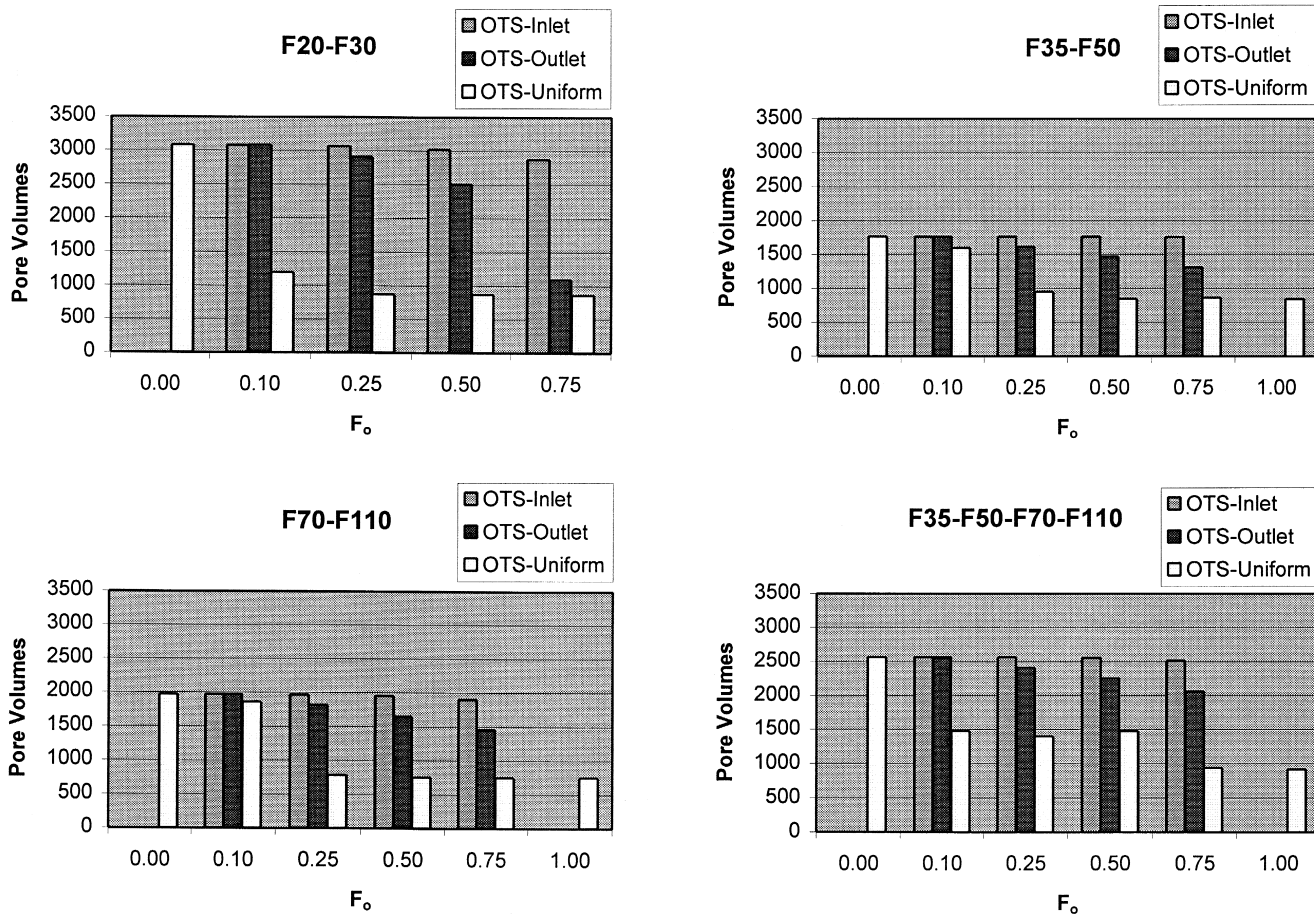


Fig. 8. A summary of the number of pore volumes required to achieve an effluent concentration four orders of magnitude below the equilibrium solubility for PCE entrapped in the various wettability distribution systems.

systems. Several trends are discernable in Fig. 8. First, note that, for a given soil and wettability distribution, increasing the NAPL-wet fraction results in a decreased remediation time. For a given column-averaged fractional wettability, the OTS-uniform system exhibits the fastest remediation time, followed by the OTS-outlet, and finally, the OTS-inlet systems. Also, observe that the difference between the remediation time for the OTS-inlet and OTS-outlet systems tends to increase with increasing OTS percentage. Finally, notice that the above trends are also functions of the grain size distribution characteristics.

The shape of the effluent concentration curves (Fig. 7) and remediation times (Fig. 8) can be explained in terms of the dissolution parameters (α and β given in Table 2) that were used in the simulations. Differences in the dissolution behavior among the various soils occur as a result of differences in α and the dependence of β on the uniformity coefficient (cf. Table 2). For a given soil (fixed α), the value(s) of β controls the dissolution behavior and remediation time. In the OTS-uniform systems, the value of β decreases as the NAPL-wet mass fraction decreases (cf. Table 2, Fig. 4, and Eq. 11) and, hence, the remediation time also decreases. In the OTS-inlet and OTS-outlet systems, the value of β ranges from 0.826 to 1.0 for the water-wet layer and is zero in the NAPL-wet layer (cf. Table 2). The dissolution behavior in these systems can be viewed as a superposition of the dissolution behavior of the two layers. The remediation times for the OTS-uniform systems are always shorter than the layered systems, due to the presence of a water-wet (larger β value) layer. Differences in the dissolution behavior of the OTS-inlet and OTS-outlet systems occur as a result of differences in the upstream concentration history. In the OTS-inlet systems, water passing through the NAPL-wet layer rapidly achieves high concentrations and, hence, the entrapped PCE in the water-wet layer is relatively unaffected until the NAPL-wet layer is “completely” remediated. At this time, an inflection point in the effluent concentration curve is observed (cf. Fig. 7). In the OTS-outlet case, the upstream concentration of water passing into the NAPL-wet layer is not always at a high value and, hence, both water-wet and NAPL-wet layers can be remediated simultaneously. As dissolution progresses, the downstream NAPL-wet layer can actually be remediated before the upstream water-wet layer. At this time, an inflection point in the effluent concentration curve is observed (cf. Fig. 7). As the size of the water-wet layer increases (decreasing OTS percent), the difference in remediation time between OTS-inlet and OTS-outlet systems increases.

7. Summary and conclusions

This paper explores the mathematical modeling of residual PCE dissolution in fractional wettability porous media. A one-dimensional solute transport simulator (MGANGLIA) was developed that incorporates rate-limited dissolution and desorption using linear driving force expressions. This model was subsequently employed to analyze the dissolution data of Bradford et al. (1999) and to explore the influence of spatial distributions of wettability on PCE dissolution.

Published mass transfer correlations describe the dissolution behavior of organic liquids entrapped in water-wet media. The use of these correlations in conjunction with MGANGLIA revealed that no single correlation was able to provide a good prediction for all of the water-wet dissolution data. Reasonable agreement between the dissolution data and simulation results was obtained, however, when application of a correlation was restricted to grain sizes consistent with its development. This observation highlights the fact that dissolution correlations are only valid for the experimental parameter ranges for which they were developed.

All of the published dissolution correlations neglect wettability considerations and were unable to capture the effluent concentration behavior of fractional wettability systems. Consequently, a simple two-parameter power function correlation for the modified Sherwood number was developed and utilized to describe each fractional wettability dissolution dataset. Model parameters were fit to the dissolution data using a nonlinear least squares fitting routine, in conjunction with the dissolution simulator. Good model fits were achieved for both water- and NAPL-wet soils. The two-parameter correlation, however, failed to capture the observed inflection point in effluent concentration curves of some of the low NAPL-wet fraction systems. For such systems, only the average dissolution behavior could be captured by this simple two-parameter model.

Correlations between model fitting parameters and wettability and grain size distribution characteristics were developed. An application of the resulting modified Sherwood model was found to yield good predictions for the dissolution behavior of the higher NAPL-wet fraction systems. Predictions for the lower NAPL-wet fraction systems were, however, often less satisfactory. This behavior was attributed to the increased sensitivity of the simulation results to variations in β at higher values of this exponent, which occur in these lower NAPL-wet fraction systems.

After recovery of the vast majority of separate phase PCE, low concentration tailing was observed in many of the fractional wettability dissolution experiments. The magnitude and duration of the concentration rebounds, following extended periods of flow interruption, indicate that only very small amounts of separate phase PCE remained in several of the lower NAPL-wet fraction systems. Numerical simulations which employed equilibrium sorption parameters in conjunction with a fitted desorption rate coefficient were able to successfully describe the remaining low concentration tailing data. Hence, rate-limited desorption is likely an important factor in the complete recovery of PCE from these fractional wettability systems.

Numerical experiments were conducted to explore the influence of spatial variations in wettability on PCE dissolution. Results indicate that both the magnitude and spatial distribution of wettability strongly influence dissolution behavior. In general, increasing the magnitude of the soil NAPL-wet fraction resulted in a decrease in the remediation time. This lower remediation time was most pronounced in systems having a uniform distribution of water-wet and NAPL-wet solids. Layering tended to substantially increase remediation time for a given level of fractional wettability. In such layered systems, the long-term dissolution behavior and remediation time were controlled by remediation of the water-wet layer.

There is currently little information available on natural subsurface variations in soil wetting properties. Results presented herein suggest that wettability characteristics can

have a marked influence on NAPL persistence. Hence, there is a need to quantify wettability parameters in natural soils and subsurface formations. In this work, the value of the NAPL-wet fraction of the soil was known and equal to the OTS-treated sand mass fraction. For natural soils, it may be possible to correlate traditional wettability indices with known OTS fraction to provide a relatively simple means of estimating the “equivalent” OTS fraction of a particular soil (cf., Bradford and Leij, 1995). Future research will investigate the dissolution of organic liquids entrapped in natural soils, and the application of these findings to larger scale aquifer environments.

Acknowledgements

The authors would like to thank David Doezema for measuring the batch sorption data for this work. Funding for this research was provided by the National Institute of Environmental Health Sciences under Grant #ES04911. The research described in this article has not been subject to Agency review and, therefore, does not necessarily reflect the views of the Agency, and no official endorsement should be inferred.

References

- Abriola, L.M., Pennell, K.D., Weber, W.J. Jr., Lang, J.R., Wilkins, M.D., 1999. Persistence and interphase mass transfer of organic contaminants in the unsaturated zone: experimental observations and mathematical modeling. In: Parlange, J.Y., Hopmans, J.W. (Eds.), *Vadose Zone Hydrology: Cutting Across Disciplines*. Oxford Univ. Press, New York, pp. 210–234.
- Anbeek, C., 1993. The effect of natural weathering on dissolution rates. *Geochim. Cosmochim. Acta* 57, 4963–4975.
- Anderson, W.G., 1986. Wettability literature survey: Part 1. Rock/oil/brine interactions and the effects of core handling on wettability. *J. Pet. Technol.* 38, 1125–1144.
- Ball, W.P., Roberts, P.V., 1991. Long-term sorption of halogenated organic chemicals by aquifer material: Part 2. Intraparticle diffusion. *Environ. Sci. Technol.* 25, 1237–1249.
- Bear, J., 1972. *Dynamics of Fluids in Porous Media*. Dover, New York.
- Borden, R.C., Kao, C.-M., 1992. Evaluation of groundwater extraction for remediation of petroleum-contaminated aquifers. *Water Environ. Res.* 64, 28–36.
- Bradford, S.A., Vendlinski, R.A., Abriola, L.M., 1999. The entrapment and long-term dissolution of tetrachloroethylene in fractional wettability porous media. *Water Resour. Res.* 35, 2955–2964.
- Bradford, S.A., Leij, F.J., 1995. Fractional wettability effects on two- and three-fluid capillary pressure–saturation relations. *J. Contam. Hydrol.* 20, 89–109.
- Bradford, S.A., Leij, F.J., 1997. Estimating interfacial areas for multi-fluid soil systems. *J. Contam. Hydrol.* 27, 83–105.
- Brown, R.J.S., Fatt, I., 1956. Measurements of fractional wettability of oilfield rocks by the nuclear magnetic relaxation method. *Trans. Am. Inst. Min., Metall. Pet. Eng.* 207, 262–264.
- Brown, C.E., Neustadter, E.L., 1980. The wettability of oil/water/silica systems with reference to oil recovery. *J. Can. Pet. Technol.* 19, 100–110.
- Brown, C.L., Pope, G.A., Abriola, L.M., Sepehrnoori, K., 1994. Simulation of surfactant-enhanced aquifer remediation. *Water Resour. Res.* 30, 2959–2977.
- Carter, M.C., Kilduff, J.E., Weber, W.J. Jr., 1995. Site energy distribution analysis of preloaded adsorbents. *Environ. Sci. Technol.* 29, 1773–1780.

- DeBano, L.F., 1969. Water repellent soils: a worldwide concern in management of soil and vegetation. *Agric. Sci. Rev.* 7, 11–18.
- DeBano, L.F., 1981. Water repellent soils: A state of the art. Gen. Tech. Rep. PSW-46, Pac. Southwest For. and Range Exp., Stn., US Department of Agriculture, Berkeley, CA.
- Dekker, L.W., Ritsema, C.J., 1994. How water moves in a water repellent sandy soil: Part 1. Potential and actual water repellency. *Water Resour. Res.* 30, 2507–2519.
- Donaldson, E.C., Thomas, R.D., Lorenz, P.B., 1969. Wettability determination and its effect on recovery efficiency. *Soc. Pet. Eng. J.* 9, 13–20.
- Dubey, S.T., Doe, P.H., 1993. Base number and wetting properties of crude oils. *SPE Reservoir Eng.* 9, 195–200.
- Geller, J.T., Hunt, J.R., 1993. Mass transfer from nonaqueous phase organic liquids in water-saturated porous media. *Water Resour. Res.* 29, 833–846.
- Hayduk, W., Laudie, H., 1974. Prediction of diffusion coefficients for nonelectrolytes in dilute aqueous solutions. *AIChE J.* 20, 611–615.
- Hirasaki, G.J., 1991. Wettability: fundamentals and surface forces. *SPE Form. Eval.* 6, 217–226.
- Hunt, J.R., Sitar, N., Udell, K.S., 1988. Nonaqueous phase liquid transport and cleanup: Part 1. Analysis of mechanisms. *Water Resour. Res.* 24, 1247–1258.
- Imhoff, P.T., Arthur, M.H., Miller, C.T., 1998. Complete dissolution of trichloroethylene in saturated porous media. *Environ. Sci. Technol.* 32, 2417–2424.
- Imhoff, P.T., Jaffe, P.R., Pinder, G.F., 1994. An experimental study of complete dissolution of a nonaqueous phase liquid in a saturated porous media. *Water Resour. Res.* 30, 307–320.
- Imhoff, P.T., Frizzell, A., Miller, C.T., 1997. Evaluation of thermal effects on the dissolution of a nonaqueous phase liquid in porous media. *Environ. Sci. Technol.* 31, 1615–1622.
- Imhoff, P.T., Miller, C.T., 1996. Dissolution fingering during the solubilization of nonaqueous phase liquids in saturated porous media: Part 1. Model predictions. *Water Resour. Res.* 32, 1919–1928.
- Kavanaugh, M.C., 1996. Contaminant site remediation — technology versus public-policy. *Water Environ. Res.* 68, 963–964.
- Lamarche, P., 1991. Dissolution of immiscible organics in porous media, PhD thesis, University of Waterloo, Ontario, Canada.
- Letej, J., Osborn, J.F., Valoras, N., 1975. Soil Water Repellency and the Use of Nonionic Surfactants. Contribution 154. California Water Resource Center, Davis, CA.
- Levenberg, K., 1944. A method for the solution of certain non-linear problems in least squares. *Q. Appl. Math.* 2, 164–168.
- Lide, D.R., 1994. CRC Handbook of Chemistry and Physics, 5th edn. CRC Press, Boca Raton, FL.
- Lorenz, P.B., Donaldson, E.C., Thomas, R.D., 1973. Use of centrifugal measurements of wettability to predict oil recovery. Report 7873, US Bureau of Mines, Bartlesville Energy Technology Center, Bartlesville, OK.
- Ma'shum, M., Tate, M.E., Jones, G.P., Oades, J.M., 1988. Extraction and characterization of water-repellent materials from Australian soils. *J. Soil Sci.* 39, 99–109.
- Mackay, D.M., Cherry, J.A., 1989. Groundwater contamination: pump- and -treat remediation. *Environ. Sci. Technol.* 23, 630–636.
- Marquardt, D.W., 1963. An algorithm for least-squares estimation of nonlinear parameters. *J. Soc. Ind. Appl. Math.* 11, 431–441.
- Mercer, J.W., Skipp, D.C., Giffin, D., 1990. Basics of Pump- and -Treat Ground-Water Remediation Technology. United State Environmental Protection Agency, R.S. Kerr Environmental Research Lab, Ada, OK.
- Miller, C.T., Poirier-McNeill, M.M., Mayer, A.S., 1990. Dissolution of trapped nonaqueous phase liquids: mass transfer characteristics. *Water Resour. Res.* 26, 2783–2796.
- Miller, C.T., Christakos, G., Imhoff, P.T., McBride, J.F., Pedit, J.A., Trangenstein, J.A., 1998. Multiphase flow and transport modeling in heterogeneous porous media: challenges and approaches. *Adv. Water Resour.* 21, 77–120.
- Morrow, N.R., 1975. The effects of surface roughness on contact angle with special reference to petroleum recovery. *J. Can. Pet. Technol.* 14, 42–53.
- Morrow, N.R., 1976. Capillary pressure correlations for uniformly wetted porous media. *J. Can. Pet. Technol.* 15, 49–69.

- Morrow, N.R., Mungan, N., 1971. Wettability and capillarity in porous media. Report RR-7, Petroleum Reservoir Research Institute, Calgary, Canada.
- Murphy, E.M., Zachara, J.M., Smith, S.C., Phillips, J.L., 1992. The sorption of humic acids to mineral surfaces and their role in contaminant binding. *Sci. Total Environ.* 117/118, 413–423.
- Myers, R.H., 1986. *Classical and Modern Regression with Applications*. Duxbury Press, Boston, MA.
- Parker, J.C., Katyal, A.K., Kaluarachchi, J.J., Lenhard, R.J., Johnson, T.J., Jayaraman, K., Jayaraman, K., Unlu, K., Zhu, J.L., 1991. Modeling multiphase organic chemical transport in soils and ground water. Final report, EPA/600/2-91/042, US Environment Protection Agency, Washington, D.C.
- Penman, H.C., 1940. Gas and vapor movement in soils. *J. Agric. Sci.* 30, 437–462.
- Pennell, K.D., Abriola, L.M., Weber, W.J. Jr., 1993. Surfactant-enhanced solubilization of residual dodecane in soil columns: Part I. Experimental investigations. *Environ. Sci. Technol.* 27, 2332–2340.
- Powers, S.E., Loureiro, C.O., Abriola, L.M., Weber, W.J. Jr., 1991. Theoretical study of the significance of nonequilibrium dissolution of nonaqueous phase liquids in subsurface systems. *Water Resour. Res.* 27, 463–477.
- Powers, S.E., Abriola, L.M., Weber, W.J. Jr., 1992. An experimental investigation of NAPL dissolution in saturated subsurface systems: steady state mass transfer rates. *Water Resour. Res.* 28, 2691–2705.
- Powers, S.E., Abriola, L.M., Weber, W.J. Jr., 1994a. An experimental investigation of NAPL dissolution in saturated subsurface systems: transient mass transfer rates. *Water Resour. Res.* 30, 321–332.
- Powers, S.E., Abriola, L.M., Dunkin, J.S., Weber, W.J. Jr., 1994b. Phenomenological models for transient NAPL-water mass-transfer processes. *J. Contam. Hydrol.* 16, 1–33.
- Salathiel, R.A., 1973. Oil recovery by surface film drainage in mixed wettability rocks. *J. Pet. Technol.* 25, 1216–1224.
- Samuels, M.L., 1989. *Statistics for the Life Sciences*. Collier Macmillan Publishers, London, UK.
- Testa, S.M., Winegardner, D.L., 1991. *Restoration of Petroleum Contaminated Aquifers*. Lewis Publishers, Chelsea, MI.
- Thomas, M.M., Clouse, J.A., Longo, J.M., 1993. Adsorption of organic compounds on carbonate minerals: Part I. Model compounds and their influence on mineral wettability. *Chem. Geol.* 109, 201–213.
- Wang, F.H.L., 1988. Effect of wettability alteration on water/oil relative permeability, dispersion and flowable saturation in porous media. *SPE Reservoir Eng.* 4, 617–628.
- Wang, H.L., Guidry, L.J., 1994. Effect of oxidation–reduction condition on wettability alteration. *SPE Form. Eval.* 9, 140–148.
- Weber, W.J. Jr., McGinley, P.M., Katz, L.E., 1991. Sorption phenomena in subsurface systems: concepts, models and effects on contaminant fate and transport. *Water Res.* 25, 499–528.
- Weber, W.J. Jr., DiGiano, F.A., 1996. *Process Dynamics in Environmental Systems*. Wiley, New York, NY.
- Wilson, J.L., Conrad, S.H., Mason, W.R., Peplinski, W., Hagan, E., 1990. Laboratory investigation of residual liquid organics from spills, leaks and the disposal of hazardous wastes in groundwater. Final report, EPA/600/6-90/004, US Environmental Protection Agency, Washington, DC.
- Wu, S., Gschwend, P.M., 1986. Sorption kinetics of hydrophobic organic compounds to natural sediments and soils. *Environ. Sci. Technol.* 20, 717–725.
- Zheng, J., Powers, S.E., 1999. Organic bases in NAPLs and their impact on wettability. *J. Contam. Hydrol.* 39, 161–181.